communications sustainability

Article

A Nature Portfolio journal

https://doi.org/10.1038/s44458-026-00035-9

Comparative assessment of United States coastal hubs for large scale electrochemical marine carbon dioxide removal

Abdelrahman Refaie [1], Mohsen Afshari [1], Vanessa Tapia [2], Erika La Plante [3], David Jassby [4], Gaurav Sant[4,5,6,7] & Mim Rahimi [1,8]

Removing carbon dioxide from the atmosphere is essential to meet climate targets and limit global warming. Oceans already absorb a large share of carbon dioxide, and electrochemical methods can strengthen this process by treating seawater to increase its storage capacity. Here, we identify locations along the United States coastline that can support large-scale deployment of such systems. Thirty-eight facilities with seawater intake, including power plants, desalination plants, and liquefied natural gas terminals, are grouped into five hubs: Northeast, Southeast, South, West, and Northwest. A decision-making framework evaluates each hub based on removal capacity, cost, energy mix, local emissions, community vulnerability, facility diversity, and supporting infrastructure. The South, West, and Northeast hubs rank highest for deployment because they combine strong removal potential, affordability, and infrastructure readiness. This framework provides a practical tool for selecting priority sites and guiding technology development and policy for ocean-based carbon dioxide removal.

The Intergovernmental Panel on Climate Change (IPCC) has emphasized the urgent need to reduce global CO_2 emissions to mitigate the impacts of climate change and limit global warming to below 2 °C by the end of this century[1]. Among the strategies for emissions reduction, carbon capture and storage (CCS) has been highlighted by the IPCC as a critical technology. CCS captures CO_2 emissions from point sources, such as industrial flue gases, preventing their release into the atmosphere[2,3]. The captured CO_2 is subsequently stored, e.g., in sub-surface geological reservoirs, thereby offering an approach for emissions mitigation. However, challenges with the scale-up and scale-out of CCS technologies, and associated infrastructure gaps (e.g., pipelines) are making it increasingly necessary to create new pathways for CO_2 mitigation, for point-source emitters, and by the direct removal of accumulated (excess) CO_2 from the atmosphere[4].

In particular, carbon dioxide removal (CDR) technologies remove accumulated (excess, i.e., present and forthcoming) CO_2 from the atmosphere, addressing historical emissions that CCS cannot address[4–6]. In addition, CDR provides a pathway to offset emissions from hard-to-abate sectors, enabling potential net-negative emissions, which is critical to meet longer-term climate goals (i.e., reducing atmospheric CO_2 concentrations)[5,6]. Conventional CDR methods, such as afforestation and reforestation and soil carbon sequestration, rely on natural processes to capture and store atmospheric CO_2[7]. While these approaches are well-established, their effectiveness is often limited by land availability and competition with agricultural production[8,9]. In contrast, engineered CDR solutions, such as bioenergy with carbon capture and storage (BECCS) and direct air capture (DAC), are suggested to overcome many of the limitations associated with natural processes[10]. These technologies require significantly less land, can be deployed widely, operate continuously, and are designed for durable CDR[11]. Among engineered solutions, DAC has gained prominence[12,13]. DAC combines chemical and physical methods to extract

[1]Department of Civil and Environmental Engineering, University of Houston, Houston, TX, USA. [2]Department of Earth and Environmental Engineering, Columbia University, New York, NY, USA. [3]Department of Materials Science and Engineering, University of California, Davis, Davis, CA, USA. [4]Department of Civil and Environmental Engineering, University of California, Los Angeles, CA, USA. [5]Institute for Carbon Management (ICM), University of California, Los Angeles, Los Angeles, CA, USA. [6]California Nanosystems Institute (CNSI), University of California, Los Angeles, Los Angeles, CA, USA. [7]Department of Materials Science and Engineering, University of California, Los Angeles, Los Angeles, CA, USA. [8]Materials Science and Engineering Program, University of Houston, Houston, TX, USA. e-mail: mrahimi@uh.edu

and store atmospheric CO_2 and can be powered by renewable energy, offering a promising pathway for CDR. Despite its advantages, DAC faces significant challenges, particularly in terms of cost and the uncertainty around access to storage sites to sequester the captured CO_2[14–18].

Geological subsurface sequestration of captured CO_2 is often suggested as the preferred method for long-term storage. In geological sequestration, CO_2 is injected into saline aquifers, depleted oil and gas reservoirs, or other appropriate "pore spaces". While the technical potential of subsurface storage is enormous, the risks of leakage (e.g., due to fault activation, porous layers, cracks in capping layers, etc.) can result in CO_2 escape back into the atmosphere[19]. Thus, storage sites are likely geographically constrained and must be monitored continuously to make sure no leakage occurs, which prolongs the liability of using geological sequestration to store captured CO_2[20]. The high cost of DAC primarily arises from the CO_2 desorption step, and the need for large absorbers and blowers to move air through the system[21,22]. Research on DAC is highly active, focusing on designing more efficient and cost-effective processes to leverage this CDR technology for achieving emission reduction goals.

Marine-based CDR (mCDR) has recently drawn attention as a promising engineered carbon removal approach. mCDR leverages the ocean's role as the largest "at-the-Earth's surface" sink for CO_2, having dissolved inorganic carbon (DIC) concentrations ~140 times higher (mass per unit volume) than ambient air[23]. Moreover, not only do the oceans naturally remove ~30% of anthropogenic CO_2 emissions, annually, but the oceans store ~6 times more CO_2 than the remaining storage systems (land, atmosphere) available on the earth's surface[24,25]. The oceans naturally store CO_2 in two main forms: mineral carbonates (e.g., $CaCO_3$) and dissolved bicarbonate anions (HCO_3^-), with the latter being predominant[26]. The primary goal of mCDR systems is to enhance the ocean's and/or seawater's capacity to absorb and store additional atmospheric CO_2, making mCDR an indirect air capture technology. mCDR technologies can be broadly categorized into biological and non-biological methods[23,27]. Biological approaches utilize marine organisms, including coastal flora and primary producers, to sequester dissolved CO_2 in the ocean. Techniques in this category include marine BECCS[28], blue carbon enhancement[29], ocean fertilization[30], and artificial upwelling[31], all of which support CO_2-fixating organisms to eventually increase oceanic CO_2 uptake from the atmosphere. Non-biological approaches rely on activating carbonate chemistry and making use of oceanic hydrodynamics to enhance CO_2 absorption and storage. Non-biological mCDR technologies have recently received increasing attention, primarily on account of the development of electrochemical approaches as effective, efficient, and scalable approaches[23,27,32]. A similar trend has been observed in leveraging electrochemical processes for point-source CCS[6,33–41], further validating the potential of this emerging route.

Electrochemical mCDR (e-mCDR) technologies can be broadly grouped into three main pathways: direct ocean capture (DOC)[42], ocean alkalinity enhancement (OAE)[43], and hybrid methods which involve elements of both[44,45]. All these methods result in additional CO_2 uptake from the atmosphere as described by Henry's law gas-liquid equilibrium. DOC includes a range of electrochemical processes designed to remove CO_2 from seawater, by lowering or raising its pH[46,47]. In one approach, DOC involves acidifying seawater to shift the carbonate equilibrium, converting DIC into dissolved CO_2 gas that can be extracted and subsequently stored or utilized. Although less common, DOC can be alternatively implemented by increasing the pH of seawater, which promotes the conversion of DIC into carbonate ions and leads to the precipitation of carbonate minerals, such as calcium and magnesium carbonates, sequestering CO_2 in a solid form[23,48]. In parallel, OAE focuses on increasing seawater alkalinity to stimulate the natural absorption of atmospheric CO_2, converting it into stable bicarbonate and carbonate ions for long-term storage[49,50]. A comprehensive explanation of the electrochemical processes involved in CO_2 removal from seawater and the critical role of pH manipulation is provided in Section S1.1 in the Supplementary Information. Hybrid systems, such as those suggested by La Plante et al[44,45]., and pioneered by Equatic Inc., integrate features of both DOC and OAE by using electrolysis to drive pH changes, enabling the production of solid carbonate precipitates while enhancing CO_2 storage in the form of dissolved bicarbonate ions. Recently, DOC and hybrid approaches have garnered the most attention due to their operational flexibility, and ability to create valuable co-products (e.g., green hydrogen in the case of Equatic)[23,44,51]. As prominent examples of ongoing commercial activities in this space, Equatic is developing a hybrid pathway, Captura is focusing on DOC, while Planetary Technologies and Ebb Carbon are focused on OAE[23] (Section S1.2 in the Supplementary Information).

Electrochemical pH alteration, which underpins both DOC and hybrid systems, is fundamentally driven by proton-coupled electron transfer (PCET) reactions[23,52]. DOC primarily utilizes electrodialysis, often with bipolar membranes, to drive the separation of acid and base streams from seawater[42,48,53]. In bipolar membrane electrodialysis (BMED), PCET reaction causes water dissociation at the membrane interface, generating protons (acid) and hydroxide ions (base)[53]. The acidified stream shifts the carbonate equilibrium to release dissolved CO_2 as a gas, which can then be captured and sequestered, while the base stream can be used to restore alkalinity before discharge[53] or to promote the precipitation of carbonate minerals[54,55]. In contrast, the hybrid pathway relies on PCET-based electrolysis via the water splitting reaction. Water splitting to produce alkaline and acidic streams produces H_2 at the cathode, increasing pH, and evolves oxygen and/or chlorine gases at the anode, decreasing seawater pH[6,23]. A recent implementation of the hybrid process used oxygen-selective electrodes to suppress chlorine evolution that is otherwise endemic to direct seawater electrolysis[45].

While electrodialysis can operate at lower theoretical energy requirements, electrolysis-based hybrid systems offer several compelling advantages for large-scale e-mCDR applications. One major benefit is that electrolysis can be performed directly on raw seawater with minimal filtration, primarily to remove large particulates. In contrast, electrodialysis-based DOC systems require extensive pretreatment to remove divalent ions, such as Ca^{2+} and Mg^{2+}, which can cause membrane fouling, scaling, and precipitation[56]. This need for careful ion removal adds significant cost and complexity to DOC operations. Furthermore, electrolysis-based processes provide significantly higher CO_2 removal capacities; nearly 20 times greater than electrodialysis[56]. This substantial difference in throughput is critical for scaling up carbon removal to climate-relevant levels. Another notable advantage of electrolysis is the co-production of hydrogen[56], a valuable clean fuel and industrial feedstock, which can create additional revenue streams and support broader decarbonization goals. Electrodialysis-based DOC does not generate hydrogen, limiting its potential co-benefits. Additionally, hybrid systems built upon electrolysis are typically designed as closed-loop, integrated plants, which allows for straightforward measurement, reporting, and verification (MRV) of both CO_2 removal and hydrogen production[44]. In contrast, MRV is more challenging for open-system approaches, where verifying atmospheric CO_2 uptake in the ocean is less direct[57]. Finally, while electrodialysis-based DOC produces a stream of CO_2 gas that requires robust infrastructure for handling, compression, and transportation, often necessitating access to CO_2 pipelines or storage facilities[56], hybrid systems require no CO_2 infrastructure, reducing logistical complexity, especially in regions without CO_2 pipelines. Given these advantages, this paper focuses on the hybrid electrolysis-based approach. Performance data, including energetics and capture rates, are drawn from kilowatt-scale operations from Equatic, which is developing the world's largest mCDR facility employing a hybrid system[51]. A detailed comparative summary of the main e-mCDR pathways, including key performance metrics and qualitative features, is provided in Section S1.3 of the Supplementary Information

From a logistical perspective, e-mCDR systems can be deployed onshore, offshore, or on mobile platforms. Ideally, these systems operate continuously, utilizing seawater and renewable electricity as inputs. Among these three deployment scenarios, onshore systems are often the most straightforward to implement[23,27]. Onshore e-mCDR processes are designed to operate near coastlines, leveraging their proximity to both the ocean and land. Onshore facilities can be strategically located to access existing

seawater intake and outfall infrastructure, and/or CO_2 and H_2 transportation pipelines or storage infrastructure. Additionally, onshore operations offer greater flexibility in integrating a broader range of renewable energy sources[58]. Onshore e-mCDR plants can be deployed as stand-alone units or co-located with existing facilities that have seawater intake and treatment systems, such as seawater desalination plants. A recent techno-economic analysis (TEA) highlighted the potential cost benefits of co-location relative to stand-alone implementation[59]. As a result, the initial development of e-mCDR systems may focus on co-location with facilities already equipped with seawater intake and handling infrastructure.

Beyond co-location, several other factors significantly influence the effectiveness and economics of an e-mCDR plant[60,61]. The type and availability of energy sources play a critical role in determining the overall removal cost and extent. Logistics related to the handling and transportation of co-produced H_2 must also be carefully evaluated. Furthermore, social factors are important for planning the construction and operation of an e-mCDR facility. Consequently, a comprehensive assessment of these factors is necessary to evaluate the feasibility of e-mCDR systems. Additionally, while hub-based planning concepts have been developed and applied in other CDR fields (e.g., for DAC)[62–64], an analogous, systematic hub framework is currently lacking for e-mCDR. Therefore, the primary objective of this work was to identify, evaluate, and rank potential hubs along the U.S. coast for the deployment of e-mCDR systems based on hybrid approaches, leveraging existing seawater intake infrastructure and regional advantages. Figure 1 outlines the step-by-step framework used in this study to identify and rank e-mCDR hubs. We first identified coastal facilities that could potentially support co-located e-mCDR plants. These facilities include near-coastal power plants, seawater desalination plants, and liquefied natural gas (LNG) import/export facilities, all of which pump and utilize significant amounts of seawater. We then employed a hierarchical clustering technique to group geographically proximal facilities into distinct hubs along the U.S. coastline, with each hub including multiple facilities (e.g., power plants, desalination plants, and LNG terminals). Once the hubs were identified, several key factors associated with each hub were systematically evaluated. These factors included the CO_2 removal capacity of the hub, the energy supply characteristics (e.g., energy costs and the grid emission factor), H_2 management infrastructure, the local carbon footprint, the social vulnerability index, and the diversity of facility types within the hub. Multi-criteria decision-making (MCDM) methods were then applied to assign relative weights to these factors and integrate them into a systematic ranking of the hubs. Specifically, the Analytic Hierarchy Process (AHP) was used to determine the relative weight of each normalized criterion, and the Technique for Order Preference by Similarity to Ideal Solution (TOPSIS) was employed to rank the hubs based on these normalized weighted criteria. Sensitivity analysis was conducted on the AHP-derived weights, and the new weights were subsequently applied in the TOPSIS method to re-rank the hubs. Overall, this study provides a comprehensive framework for assessing and ranking the suitability of potential hubs for the large-scale deployment of e-mCDR systems. In addition to delivering overall hub rankings, the platform developed in this work offers detailed insights into the specific strengths of each hub, enabling tailored and optimized implementations of e-mCDR systems based on local conditions and infrastructure.

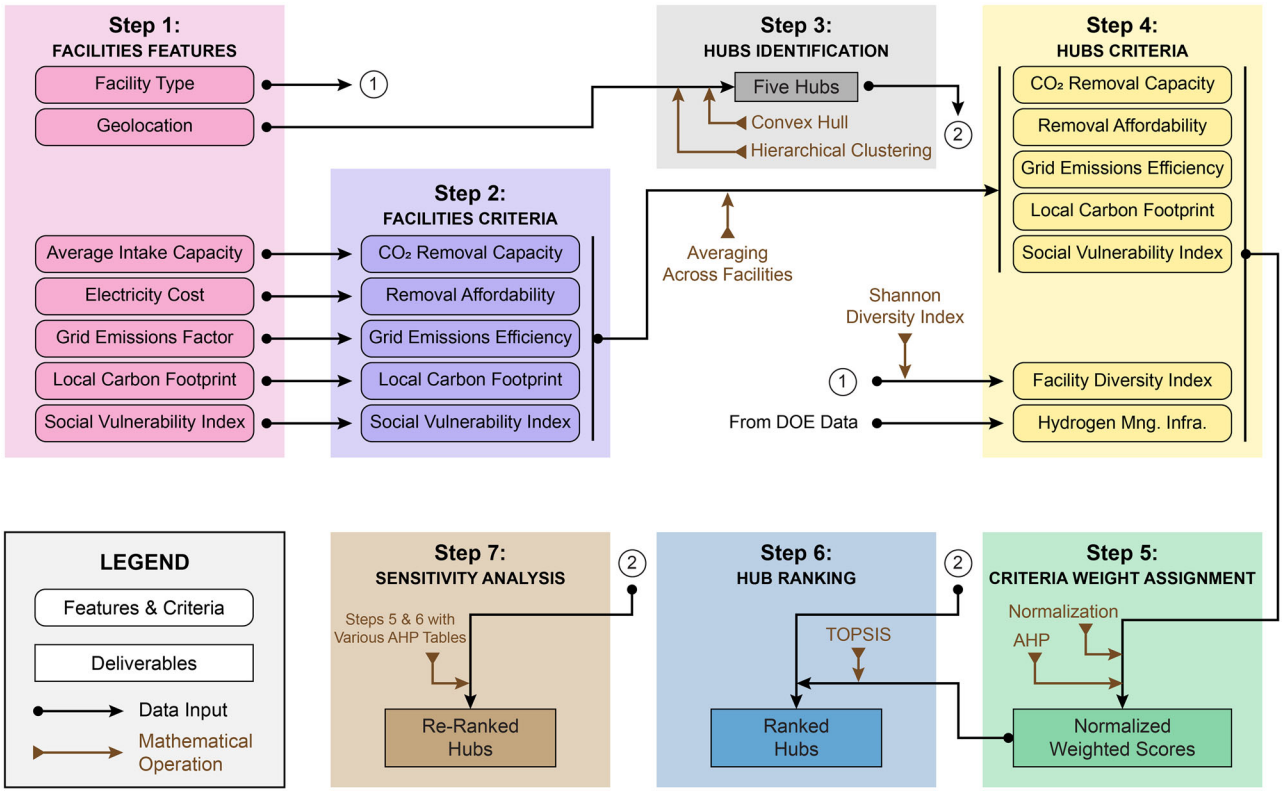

Fig. 1 | Study Framework for Identifying and Ranking e-mCDR Hubs. This study followed a logical framework to identify potential e-mCDR hubs along the U.S. coastline and rank them. **Step 1:** A total of 38 coastal facilities were identified as potential colocation sites, and a database of facility-specific features was compiled. **Step 2:** Five facility-level criteria were developed based on the collected data. **Step 3:** Hierarchical clustering (HC) was used to group geographically proximate facilities into hubs, and the Convex Hull algorithm was applied to define their geographical boundaries. **Step 4:** Two categories of hub-level criteria were established: (i) those derived from facility-level criteria and (ii) those based on hub-specific characteristics, including facility diversity index (calculated using Shannon diversity index) and hydrogen management infrastructure (adopted from the DOE Connect Data tool). **Step 5:** The Analytic Hierarchy Process (AHP) was applied to assign weights to the normalized hub-level criteria. **Step 6:** The Technique for Order Preference by Similarity to Ideal Solution (TOPSIS) was used to rank the hubs based on their normalized weighted scores. **Step 7:** A sensitivity analysis was conducted on the AHP-derived weights, and adjusted weights were applied to re-rank the hubs using TOPSIS.

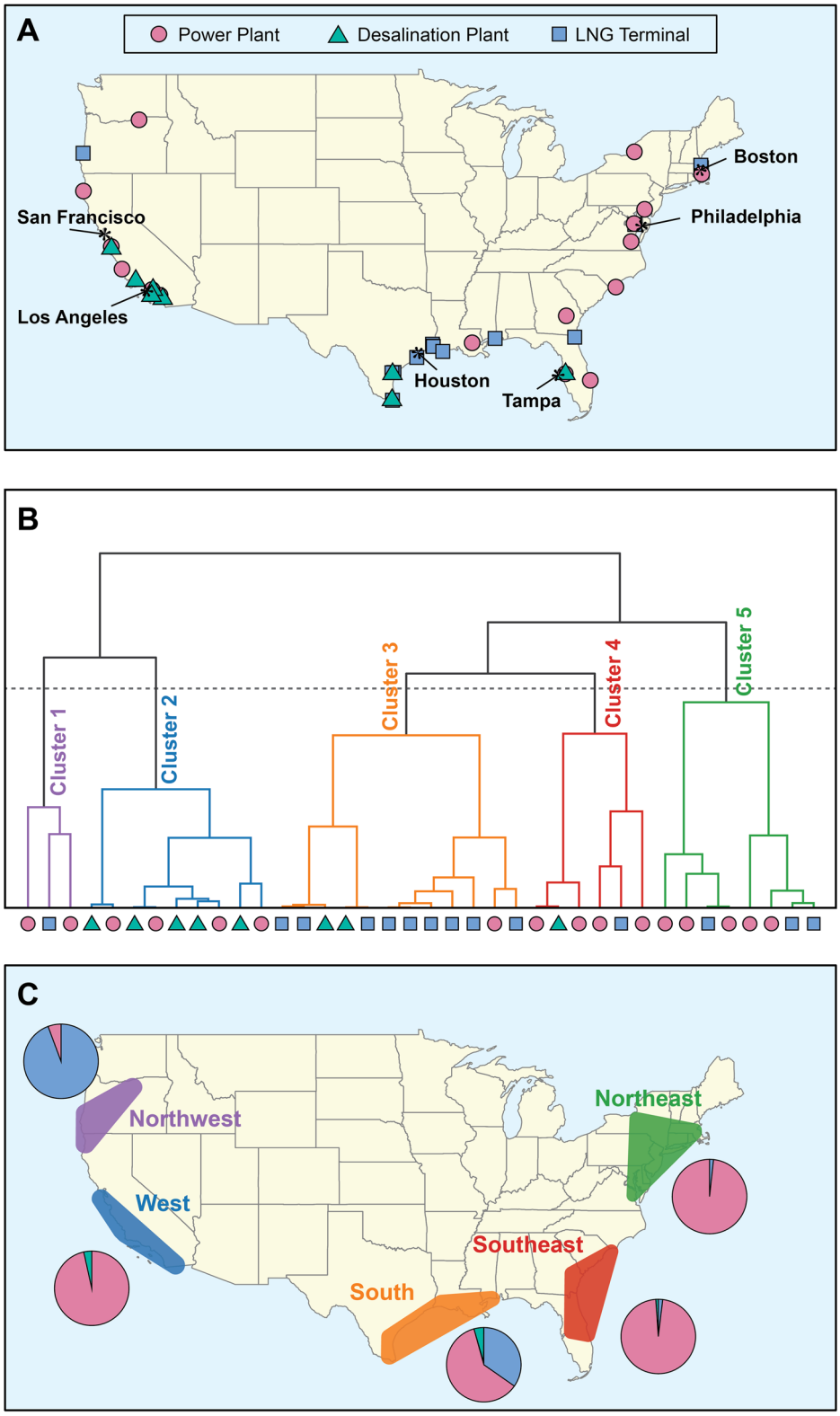

Fig. 2 | Geographical Distribution, Clustering, and Composition of Coastal e-mCDR Hubs. **A** Geographical distribution of 38 coastal facilities identified as potential colocation sites for e-mCDR deployment along the U.S. coastline. Facilities are distributed relatively uniformly, with clusters forming near major metropolitan areas. The three facility types included power plants (•), desalination plants (▲), and LNG terminals (▪). **B** Hierarchical clustering dendrogram illustrating the classification of facilities into five distinct clusters, each representing a potential e-mCDR hub based on geographical proximity. **C** Identified e-mCDR hubs and facility composition. The five hubs—Northeast, Southeast, South, West, and Northwest—are delineated using the Convex Hull algorithm. Each hub's composition is represented by a pie chart indicating the percentage distribution of power plants, desalination plants, and LNG terminals within the hub.

Results And discussion

Spatial Analysis of Coastal Facilities

An assessment of the geographical distribution of the facilities revealed important insights about their locations along the U.S. coastline. Most facilities are located near major metropolitan areas, as proximity to these cities is crucial for their operations. For example, on the West Coast, facilities are concentrated around the Greater San Francisco and Los Angeles Areas, while along the Gulf Coast, they are located in or near the Greater Houston area. Similarly, on the East Coast, facilities are situated around major cities (Fig. 2A).

A comparison of facility types across different geographic regions revealed distinct patterns. The East predominantly includes power plants, the South hosts a higher number of LNG terminals, and the West features more seawater desalination plants[65]. This distribution aligns with the unique

needs and characteristics of each region. For instance, the East's higher population density necessitates a greater number of power plants to meet electricity demands[66]. The South's abundance of LNG terminals is attributed to being located on the coast of the Gulf of Mexico, which is favorable for LNG export/import terminals[67,68]. In contrast, the West requires desalination plants to address the region's limited freshwater resources[69]. These regional variations highlight the functional specialization of facilities based on local demands and resources.

Hub Analysis

Using the HC method based on the geolocation of facilities, five distinct clusters were identified through the dendrogram, shown in Fig. 2B. These clusters correspond to five coastal regions that vary significantly in terms of economic conditions, population, and climate[70]. These regions are designated as the Northeast, Southeast, South, West, and Northwest hubs, each representing a potential e-mCDR hub. These identified hubs were illustrated on the US map using the Convex Hull method (Fig. 2C).

An initial analysis of the facility distribution within each hub reveals notable differences. The Northeast and Southeast hubs are characterized by water intake capacity predominantly from power plants, accounting for 98% and 97% of their total intake, respectively. In the South hub, power plants contribute 61% of the water intake capacity, followed by LNG terminals at 35%. Despite housing several desalination plants, power plants' water intake capacity dominates the West hub, representing 96.5% of its total water intake capacity. In contrast, the Northwest hub is unique, with 94% of its water intake capacity attributed to LNG terminals (Fig. 2C). Overall, the majority of water intake capacity across all hubs is associated with power plants, highlighting their significant water consumption compared to LNG terminals and desalination plants. Although the South and West hubs have fewer power plants, this facility type still accounts for the largest share of water intake capacity. The Northwest hub is an exception, as the lack of large fossil fuel-based power plants results in LNG terminals being the primary contributors to water intake capacity. Among the identified hubs, the South stands out as the most diverse, with a balanced mix of facility types.

Comparative Analysis of Hub Criteria

To gain deeper insights into the suitability of each hub for e-mCDR implementation, a comparative analysis was conducted based on the seven evaluation criteria previously established. Figure 3 provides a visual representation of the hubs' performance across these criteria, facilitating a comprehensive understanding of their strengths and limitations. The Northeast hub demonstrated relatively high CO_2 removal capacity, primarily attributed to the high water intake of the facilities located in this hub. The hub also offers high grid emissions efficiency, making it a viable option within the hybrid pathway to achieve net carbon negative outcomes. However, the Northeast hub ranked low in facility diversity, with power plants being the predominant colocation facilities. Considering its strengths and weaknesses, the Northeast hub is best suited for e-mCDR projects that focus on the hybrid pathway, prioritizing total CO_2 removal capacity with a net carbon negative.

The Southeast hub demonstrates high removal affordability and a favorable social vulnerability index. The relatively low electricity costs in states, such as Florida and Georgia are primarily driven by the region's reliance on cost-effective natural gas and nuclear power generation[71].

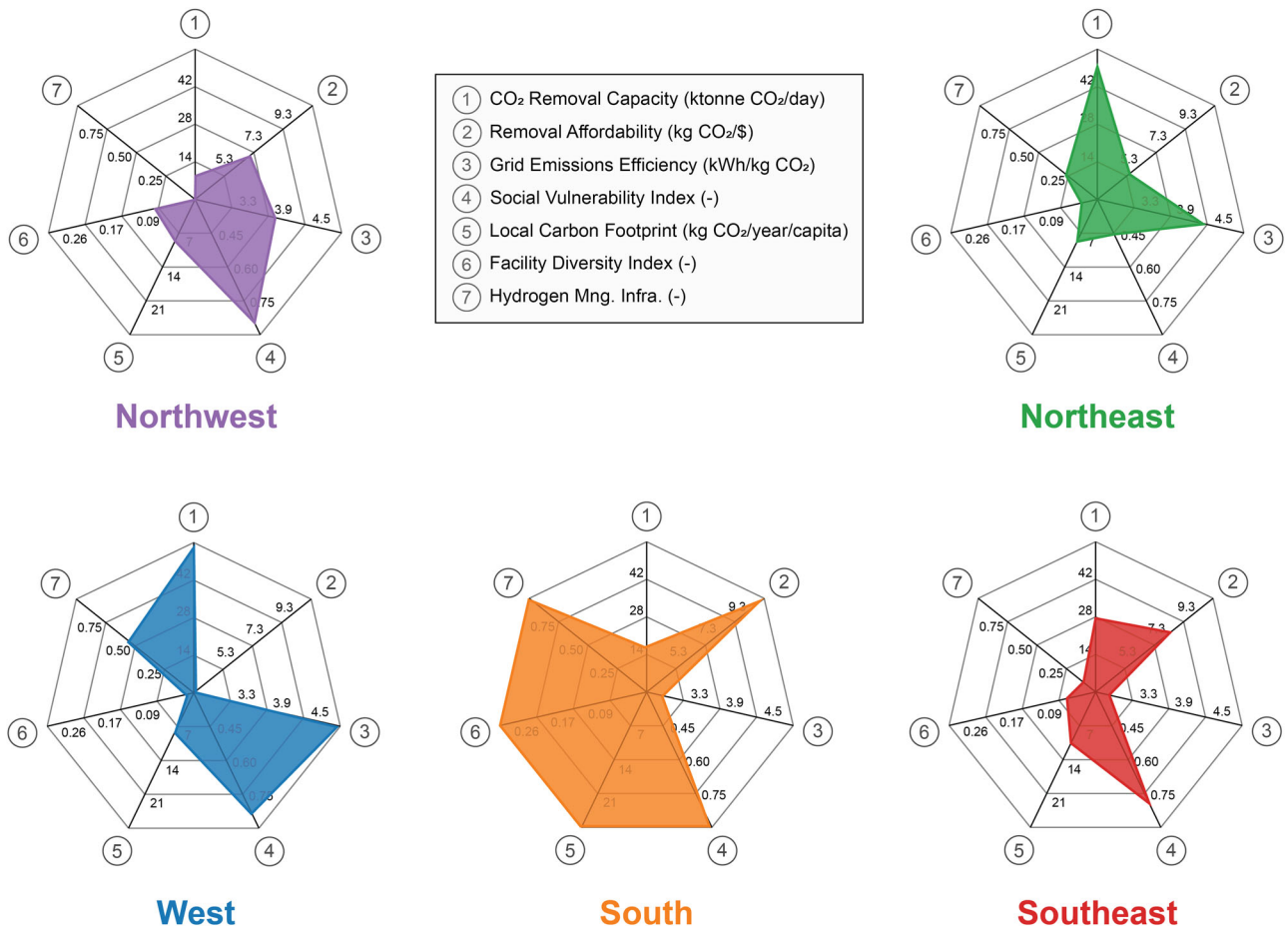

Fig. 3 | Comparative Performance of e-mCDR Hubs. Comparison of the five e-mCDR hubs across the seven hub-level criteria, highlighting their relative strengths and limitations. These criteria included CO_2 removal capacity (ktonne CO_2/day), removal affordability (kg CO_2/$), grid emissions efficiency (kWh/kg CO_2), social vulnerability index (-), local carbon footprint (kg CO_2/year/capita), facility diversity index (-), and hydrogen management infrastructure (-).

Additionally, the region exhibits a high social vulnerability index due to factors, such as higher population densities in coastal areas, economic disparities, and exposure to climate-related hazards. The hub possesses average local carbon footprint values, as the region does not host a significant number of CO_2-emitting industries. Despite these advantages, the Southeast hub faces limitations in grid emissions efficiency, with relatively low integration of clean energy sources into the grid. Furthermore, the region lacks significant hydrogen management infrastructure, which could pose challenges for implementing hydrogen-focused e-mCDR pathways.

The South hub demonstrated the highest performance across five of the evaluated criteria, including removal affordability, social vulnerability index, local carbon footprint, facility diversity index, and hydrogen management infrastructure. Similar to the Southeast hub, the South benefits from cost-effective electricity, primarily due to the widespread availability of natural gas, wind, and nuclear power generation in states, such as Texas and Louisiana[71]. The social vulnerability index is also notably high in this region, largely because many of the facilities are situated in areas designated under the Justice40 initiative[72], which aims to address environmental and economic disparities in disadvantaged communities. The South hub's high local carbon footprint is attributed to the presence of some of the largest CO_2-emitting industries in the country, primarily within the oil and gas sector[73]. Texas and Louisiana are major energy-producing states, housing numerous refineries, petrochemical plants, and processing facilities that contribute significantly to national CO_2 emissions. One of the South hub's key strengths is its high facility diversity, including power plants, desalination plants, and LNG terminals. This diversity is crucial from a logistical perspective, as it enhances the hub's adaptability to potential regulatory changes and technical challenges. For instance, if stringent environmental regulations were imposed on a specific facility type, such as desalination plants, or if retrofitting e-mCDR systems into certain process flow diagrams proved challenging, the hub's diversity would provide flexibility in selecting suitable alternative facilities for deployment, thereby mitigating logistical and technical constraints. Additionally, the South hub includes robust hydrogen management infrastructure, with Texas and Louisiana being home to some of the largest H_2 storage facilities, as well as extensive pipeline networks and transportation systems[74–76]. The region hosts several large hydrogen hubs and pipelines to meet the growing demand for H_2 as an alternative energy source[77]. The generated H_2 can also serve as valuable feedstocks for numerous industrial units located within or near the hubs, further enhancing the economic feasibility of e-mCDR deployment.

The South hub also has certain limitations that may impact its potential for e-mCDR implementation. The hub demonstrated the lowest CO_2 removal capacity among all evaluated regions. This limitation is primarily attributed to the low overall seawater intake capacity. Despite achieving a low score in grid emissions efficiency, the South hub has a sufficient score for the hybrid pathway to provide a net carbon negative result. This performance can be attributed to the region's substantial wind energy generation capacity, with Texas being the largest wind electricity producer in the United States[78]. The state has made significant investments in wind power infrastructure, contributing to a relatively higher share of renewables compared to other industrialized regions. However, fossil fuels still dominate the energy mix, with natural gas and coal remaining primary energy sources. Louisiana continues to heavily depend on fossil fuels, with minimal integration of renewable energy sources into its grid[71].

Considering all evaluated criteria, the South hub emerges as an attractive location for implementing e-mCDR technologies. Its strong removal affordability, extensive hydrogen management infrastructure, and high facility diversity collectively position it as a strategic choice for large-scale deployment. The availability of well-established industrial networks and extensive transportation infrastructure further enhances the hub's attractiveness for integrating e-mCDR with existing processes. While the Southeast hub excels in criteria, such as removal affordability and social vulnerability index, the South hub demonstrates even greater strengths in these areas. This superior performance, coupled with the geographic proximity of the two hubs, suggests that the South hub is likely to attract e-mCDR projects that would otherwise consider the Southeast.

The Western hub exhibited the highest CO_2 removal capacity among all evaluated hubs. This superior performance is attributed to the high water intake capacity of this hub. Although the cost of electricity is relatively high in this region, which lowers its removal affordability, it offers a very high clean energy capacity, mostly located in Southern and Central California, introducing substantial renewable energy sources into the grid[79]. The Western hub also benefits from well-developed hydrogen management infrastructure, providing access to existing storage facilities and transportation networks that could support e-mCDR deployment. The development of H_2 infrastructure is driven by environmental policies[80], with H_2 infrastructure being particularly focused on its use in transportation[81]. One of the primary limitations of the Western hub is its low facility diversity index, as the majority of its water intake capacity comes from power plants. This lack of diversity may introduce logistical challenges, as previously discussed, potentially limiting the hub's adaptability to regulatory changes or technical constraints associated with integrating e-mCDR systems into desalination operations.

The Northwest hub achieved a moderate score in grid emissions efficiency, with most facilities located in Northern California and Oregon, regions that have some of the highest renewable energy integration in the country[71,82]. The availability of renewable energy resources, from hydroelectric, wind, and solar power, enhances the region's potential for low-carbon e-mCDR operations. Similar to most of the hubs, the Northwest hub also ranked high in social vulnerability index, largely due to the presence of several Justice40-designated communities that can benefit from sustainable climate initiatives[72]. The hub demonstrated moderate performance in other criteria, including removal affordability, local carbon footprint, and facility diversity index. A key limitation of the Northwest hub is its underdeveloped hydrogen management infrastructure, which could hinder the integration of hydrogen-focused e-mCDR pathways and limit opportunities for utilizing captured H_2 as a feedstock for local industries, if new facilities (e.g., for Sustainable Aviation Fuels, SAFs) are not built. Given its moderate overall score, the Northwest hub remains an attractive option for implementing e-mCDR systems that prioritize low-carbon operations and sustainability goals, while further development of H_2 infrastructure would unlock additional incentives for e-mCDR deployment.

Ranking of Hubs Based on Weighted Criteria

The criteria weights were determined using the AHP method to reflect their relative importance in evaluating e-mCDR hub suitability. The results, presented in Fig. 4A, indicated that CO_2 removal capacity holds the highest weight at 24%, followed by removal affordability at 23%. Green energy share contributed 23%, while local carbon footprint contributed 12%. Hydrogen management infrastructure was weighed at 9%. The facility diversity index and social vulnerability index carried the lowest weights at 6% and 4%, respectively.

This weight distribution highlights the central importance of CO_2 removal capacity. Removal affordability closely follows in importance, given its critical impact on the economic feasibility of e-mCDR projects. The significant weighing of grid emissions efficiency highlights the growing emphasis on sustainable energy sources in carbon removal initiatives. If the grid emissions efficiency is low (i.e., energy mix used to power these mCDR approaches is largely dominated by fossil fuels), then the overall process may not be carbon negative. However, as the share of renewable energy increases over the years, the net carbon removal potential of these hubs is expected to improve. Local carbon footprint and hydrogen management infrastructure, while lower in weight, still contribute meaningfully to the overall assessment. The relatively lower weights assigned to the facility diversity index and social vulnerability index suggest that while these factors are considered, they play a less critical role in determining the suitability of e-mCDR hubs for the DOC pathway.

Analyzing the top- and lowest-performing hubs for each weighted criterion is essential for understanding the factors influencing overall hub

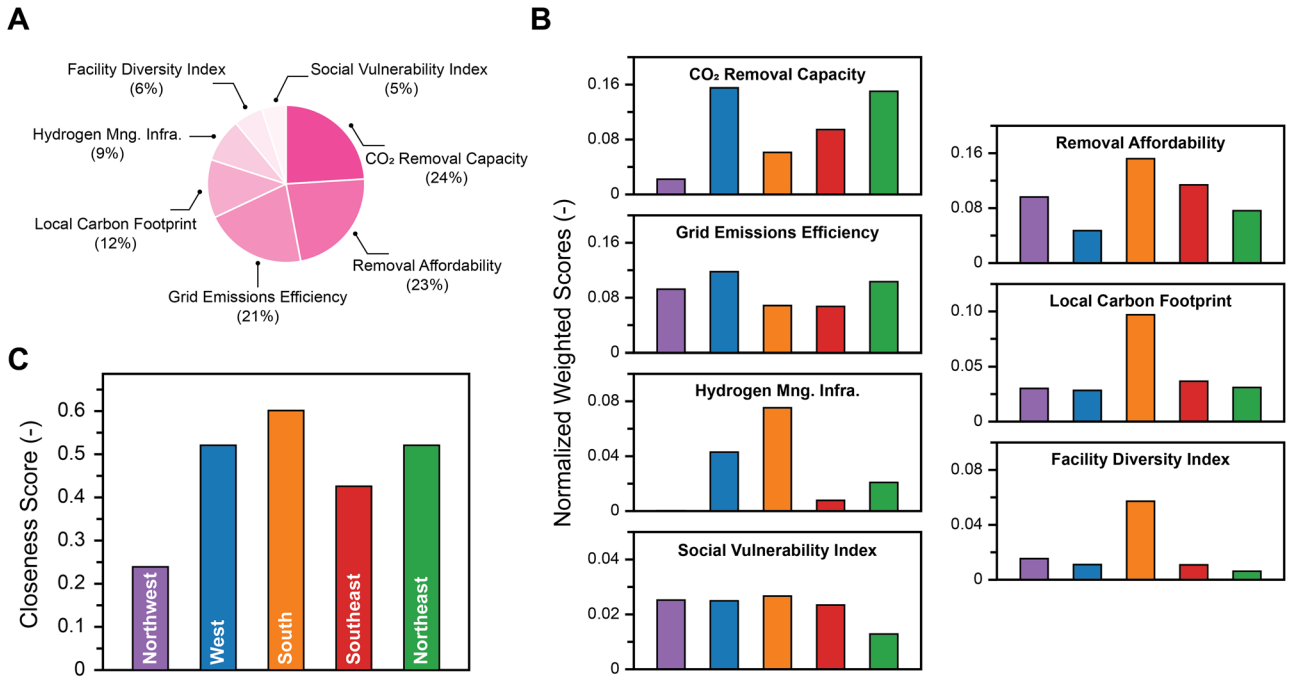

Fig. 4 | Multi-Criteria Ranking of e-mCDR Hubs. A Criteria weights assigned using the Analytic Hierarchy Process (AHP), with CO_2 removal capacity receiving the highest weight, followed by removal affordability, and grid emissions efficiency. **B** Hub rankings across individual criteria, determined using normalized weighted scores. **C** Overall hub rankings derived from the Technique for Order Preference by Similarity to Ideal Solution (TOPSIS) method, indicating that the South hub achieved the highest relative closeness score ($C = 0.60$), closely followed by the West and Northeast ($C = 0.52$).

rankings. While Fig. 3 presented the absolute scores of each criterion for the hubs, Fig. 4B illustrates the hub rankings based on normalized weighted scores determined through AHP. Regarding CO_2 removal capacity, the West and Northeast hubs outperformed the others, primarily due to their high water intake capacities. The remaining hubs exhibited relatively lower performance in this criterion. Removal affordability demonstrated substantial variability, with the South and Southeast hubs exhibiting the higher values, indicating lower electricity costs. In contrast, the grid emissions efficiency criterion showed relatively minor variation across the hubs, with the Northeast and West Coast hubs (i.e., West and Northwest) achieving slightly higher scores due to the widespread integration of renewable energy into their regional grids[83–85]. It is worth to note that all the hubs meet the grid emissions efficiency threshold for net carbon negativity which makes them suitable for e-mCDR integration[45]. In terms of the local carbon footprint, the South hub exhibited the highest score, indicating its substantial contributions to national CO_2 emissions[86]. This highlights the potential for e-mCDR implementation to achieve meaningful emission reductions in this region, whereas other hubs exhibit relatively lower emissions and may offer less immediate impact in this regard. The hydrogen management infrastructure criterion was led by the South hub, followed by the West hub, reflecting the extensive availability of H_2 transportation and storage facilities in these regions[80,81,87,88]. Additionally, the South hub stood out in the facility diversity index criterion, highlighting its broad mix of facility types, which enhances flexibility and adaptability for e-mCDR deployment. Finally, for the social vulnerability index, all hubs except the Northeast ranked high, suggesting that e-mCDR implementation in these regions could provide substantial community benefits. This further reinforces the importance of deploying such technologies in socially vulnerable areas to address environmental and economic disparities.

All weighted criteria were incorporated to rank the hubs using the TOPSIS method. The analysis revealed that the South hub achieved the highest overall relative closeness score ($C = 0.60$), closely followed by the West and Northeast hubs ($C = 0.52$). The Southeast ($C = 0.43$) and Northwest ($C = 0.24$) hubs ranked fourth and fifth, respectively (Fig. 4C). The South hub's top ranking is primarily attributed to its strong performance across multiple criteria, particularly in removal affordability, hydrogen management infrastructure, local carbon footprint, and facility diversity index. The West hub ranked highly due to its superior CO_2 removal capacity, grid emissions efficiency, and well-established hydrogen management infrastructure. Given the varied performance across the hubs, categorizing them based on their overall suitability provides a more practical perspective. Instead of a linear ranking from first to fifth, the hubs can be grouped into high potential (West, South, and Northeast), moderate potential (Southeast), and low potential (Northwest) hubs.

Sensitivity Analysis

The narrow margin between the top three hubs indicates that slight changes in the criteria's weights could influence the overall rankings. Therefore, a sensitivity analysis of the weight assignments was conducted, and the adjusted weights were subsequently applied in the TOPSIS method to re-rank the hubs. The sensitivity analysis was conducted on all seven evaluation criteria, and the results are presented in Fig. 5, highlighting the four most influential criteria impacting each hub's ranking. For the South hub, CO_2 removal capacity emerged as the most influential criterion, exerting the greatest impact on its closeness score (C). It was followed by removal affordability, local carbon footprint, and hydrogen management infrastructure, indicating the hub's reliance on these factors for maintaining its top position. Similarly, in the case of the West hub, its ranking was found to be most sensitive to the weight assigned to CO_2 removal capacity. This criterion was followed in importance by removal affordability, local carbon footprint, and facility diversity index. For the Northeast hub, the ranking was primarily influenced by CO_2 removal capacity, with local carbon footprint, removal affordability, and facility diversity index also playing significant roles. In contrast, the ranking of the Southeast hub was found to be relatively stable, with no single criterion exerting a substantial impact on their overall ranking positions. The relative closeness score for the Northwest hub is mainly impacted by the removal affordability, and CO_2 removal capacity.

For the high-potential hubs, West, South, and Northwest, which performed well across most criteria, their rankings were primarily influenced by

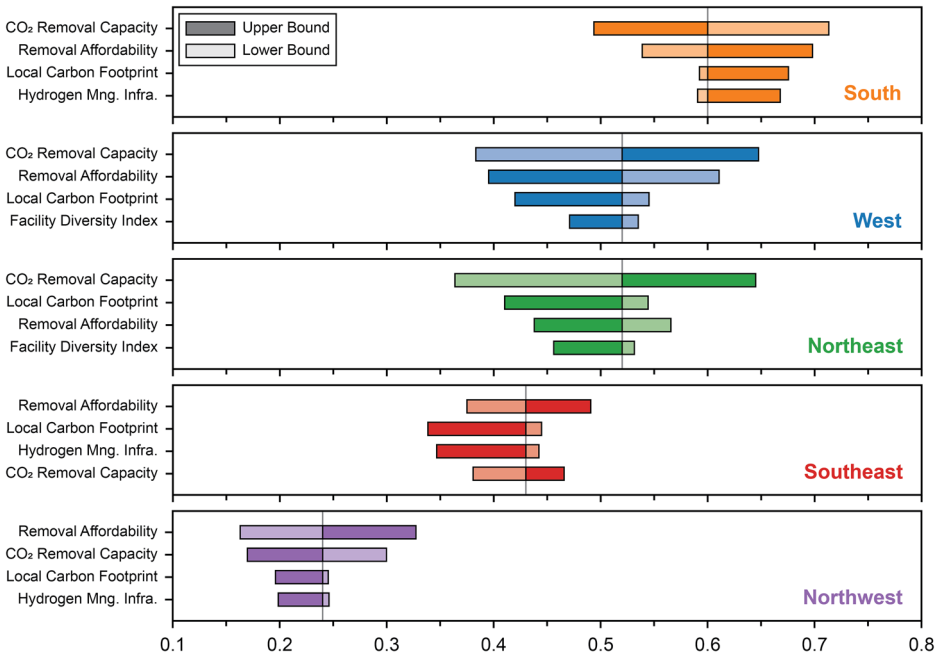

Fig. 5 | Sensitivity Analysis of Key e-mCDR Hub Criteria. Sensitivity analysis was performed on the Analytic Hierarchy Process (AHP)-derived weights to assess the impact of subjectivity in the pairwise comparison process. The analysis involved systematically adjusting the weight of each criterion by a factor of 2, both increasing (upper bound) and decreasing (lower bound), followed by recalculating the weights using AHP and re-ranking the hubs using the Technique for Order Preference by Similarity to Ideal Solution (TOPSIS). The sensitivity analysis was conducted on all seven hub-level criteria, and the results highlighted the four most influential criteria affecting each hub's ranking.

their most weighted criterion—CO_2 removal capacity. This criterion represented the primary determinant in their performance, making their rankings highly sensitive to any changes in this criterion. As a result, an improvement or deterioration in CO_2 removal capacity could significantly impact these hubs' overall standing. For instance, if the weight of CO_2 removal capacity, which reflects the relative importance of the criterion, is decreased to its lower bound, the South hub would become the single dominant hub with a C of 0.71, increasing its margin over the West ($C = 0.38$) and the Northeast ($C = 0.36$) hubs. However, if the weight is increased to its upper bound, the South hub would rank third ($C = 0.49$), after the Northeast hub ($C = 0.64$), while the West hub slightly surpasses to take first place ($C = 0.65$). The next most influential criteria were those that differentiated the most between the high-potential hubs. For instance, the South hub excelled in removal affordability, local carbon footprint, hydrogen management infrastructure, and facility diversity index, while the West and Northeast hubs struggled the most in all of these criteria. This suggests that further improvements in these criteria reinforce the South hub's competitive advantage and contribute to enhancing its overall ranking. Conversely, these criteria represent key limitations on the West and Northeast hubs' performance, acting as bottlenecks that limit their overall potential. Any improvement in these areas yields significant gains in the hub's overall ranking. For the moderate and low potential hubs, which generally perform strongly in one or two specific criteria, their rankings were primarily influenced by those criteria. For example, the rankings of the Southeast hub were most impacted by the removal affordability, as it represents its strongest criterion.

Beyond the weight-based sensitivity analysis, an additional round of sensitivity analysis was conducted to evaluate the influence of specific facility types and infrastructure characteristics on hub rankings. This analysis aimed to assess how the elimination of key facilities within each hub affects the overall ranking outcomes, providing further insight into the structural dependencies of e-mCDR deployment via the hybrid pathway. Three distinct scenarios were examined. In the first scenario (Fig. 6A), the facility with the highest water intake was removed from each hub to determine the extent to which hub rankings rely on a single high-capacity facility. Since water intake capacity directly influences CO_2 removal potential, this analysis evaluates the resilience of each hub when its largest seawater-processing facility is excluded, for example, due to logistical constraints in implementation, challenges in retrofitting, facility-specific regulatory restrictions, or potential operational disruptions. In the second scenario (Fig. 6B), all power plants were removed from each hub. Power plants generally exhibit the highest water intake capacity among the three facility types. Eliminating power plants simulates a scenario in which e-mCDR deployment is limited to smaller-scale systems that are better suited for facilities with lower water intake capacities, such as desalination plants and LNG terminals. This analysis provides insight into how hub rankings would shift under a deployment model focused on lower-capacity e-mCDR implementations rather than large-scale systems co-located with high-intake power plants. In the third scenario (Fig. 6C), all LNG terminals were removed from each hub to investigate their role in supporting e-mCDR deployment. Unlike power plants and desalination facilities, LNG terminals do not operate continuously at full capacity, and their long-term availability may be uncertain due to shifts in energy markets and policy changes[89]. This analysis assesses the extent to which hub rankings are influenced by the presence of LNG infrastructure and evaluates the potential challenges of e-mCDR deployment in hubs without LNG terminal support.

The Northwest hub exhibited the greatest sensitivity to the removal of its highest water intake facility, with a 20% decrease in its closeness score (C) compared to the base scenario, which was represented in Fig. 4C. This was followed by the South hub, which showed a 14% reduction in C. These findings suggest that the Northwest hub's ranking is disproportionately reliant on a single high-capacity facility, making its suitability for e-mCDR deployment particularly vulnerable to logistical constraints or facility-specific limitations. In contrast, the relatively lower impact observed for other hubs indicates a more distributed reliance on multiple facilities, reducing the risk associated with the unavailability of any single high-capacity site (Fig. 6; Scenario I).

The removal of power plants had a profound effect on hub rankings, with the Northeast hub experiencing the most significant decline, a 71% decrease in C, followed by the West hub, which showed a 46% reduction. This substantial drop highlights the Northeast hub's strong dependence on power plants, which account for 98% of its total water intake. Conversely, the South hub emerged as the highest-ranked hub under this scenario, with a C of 0.79, indicating that this region presents the most favorable conditions for lower-capacity e-mCDR implementations that rely on smaller seawater-processing facilities, such as desalination plants and LNG terminals (Fig. 6; Scenario II).

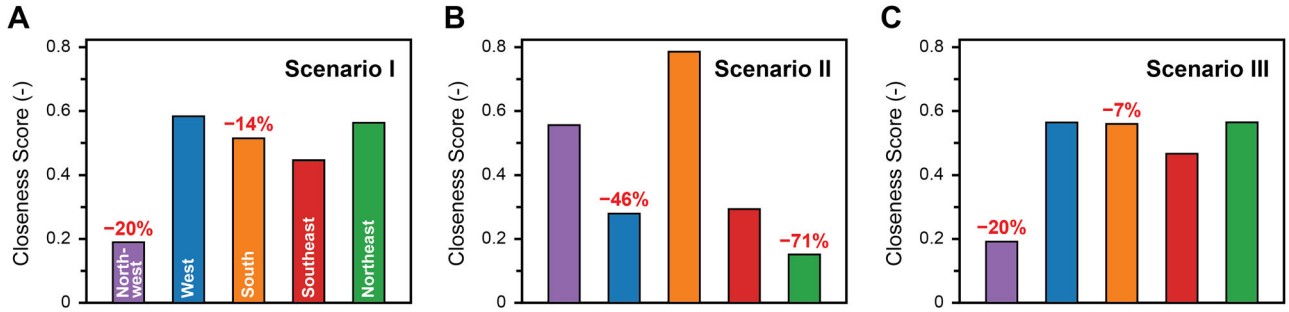

Fig. 6 | Impact of Facility-Specific Exclusions on e-mCDR Hub Rankings. Sensitivity analysis was conducted to evaluate the impact of removing specific facility types on hub rankings, providing insight into the structural dependencies of e-mCDR deployment. Closeness scores (*C*) were recalculated using the TOPSIS method for each of the following scenarios. **A** Scenario I**:** Removal of the highest water intake facility from each hub to assess the resilience of hub rankings when a single high-capacity facility is unavailable due to logistical constraints or retrofitting challenges. **B** Scenario II: Removal of all power plants from each hub to simulate a scenario where e-mCDR deployment relies solely on smaller-scale seawater-processing facilities, such as desalination plants and LNG terminals, offering insights into hub suitability for lower-capacity e-mCDR systems. **C** Scenario III: Removal of all LNG terminals from each hub to examine their influence on hub rankings, considering that LNG terminals do not operate continuously at full capacity and their long-term availability is uncertain due to shifts in energy markets and policy changes. The labels in each panel represent the two most impacted hubs for each scenario, with values indicating the percentage change in *C* relative to the base scenario.

The impact of removing LNG terminals was less pronounced than the removal of power plants, as LNG facilities generally contribute a smaller fraction of total water intake across hubs. The Northwest hub experienced the greatest reduction in ranking, with a 20% decrease in *C*, followed by the South hub, which showed a 7% decline. In this scenario, the high potential hubs (South, West, and Northeast hubs) obtained similar high ranking ($C = 0.57$), indicating that it is the most reliable for e-mCDR deployment, as LNG terminals operate intermittently and face long-term uncertainty due to shifts in energy markets and policy changes (Fig. 6; Scenario III).

The results of these scenarios provide a deeper understanding of the sensitivity of hub rankings to facility-level variations, informing future site selection and infrastructure planning for e-mCDR implementation. In general, the Northwest hub is the most susceptible to disruptions, as it exhibited the highest sensitivity across multiple scenarios, making it a relatively uncertain candidate for future e-mCDR deployment.

Future directions for e-mCDR deployment

While this study focused on identifying high-potential hubs for future e-mCDR deployment via the hybrid pathway, future research must also advance other critical aspects of the process. Key areas include further improving core electrochemical technologies and developing policy measures that ensure scalability, economic viability, and environmental justice.

To ensure e-mCDR systems are both effective and scalable, future efforts must focus on optimizing their electrochemical efficiency, durability, and modular scalability. Current efficiency—the fraction of input electricity converted into carbon removal—must be maximized to enhance energy efficiency and reduce operational costs[23,90]. Additionally, modular system designs should be developed to allow e-mCDR units to be stacked together for large-scale deployment while maintaining operational stability. Seawater presents a complex environment, posing potential durability challenges for electrochemical cell components. Electrodes, membranes, and other critical materials are susceptible to chemical degradation and fouling, particularly due to interactions with dissolved salts, organic matter, and microbial communities. Before real-world implementation, long-term stability tests under simulated marine conditions should be conducted to evaluate the resilience of system components and identify cost-effective materials with enhanced durability[91]. In parallel, refining techno-economic assessments (TEA) and life cycle analysis (LCA) will be crucial for quantifying the long-term cost-effectiveness and environmental footprint of e-mCDR projects at different hubs[91,92]. While the present work focuses on an electricity-based affordability metric to enable consistent comparison across diverse sites, future hub- and project-specific studies should integrate detailed CAPEX, O&M, and infrastructure cost components to derive full levelized costs of CO_2 removal. These assessments should incorporate regional energy costs and grid integration potential, ensuring that future deployments align with both economic and environmental sustainability targets.

Beyond technological advancements, large-scale deployment of e-mCDR requires a robust policy and regulatory framework that enhances economic viability, streamlines permitting processes, and ensures equitable implementation. Financial incentives, such as carbon credits, tax incentives, and direct subsidies are essential to improving the cost-competitiveness of e-mCDR relative to other carbon removal approaches. Public-private partnerships can play a crucial role in funding large-scale pilot and demonstration projects, facilitating collaboration between government agencies, research institutions, and industry leaders. Regulatory barriers remain a hurdle for e-mCDR deployment, particularly in marine environments where environmental permitting processes are complex and jurisdictional oversight is fragmented[93,94]. Current permitting frameworks do not fully account for electrochemical interventions in marine settings, creating uncertainty for project developers[95]. Streamlining regulatory approvals, particularly for hubs near federally controlled waters, will be critical for scaling deployment. Establishing harmonized regulations at the federal and state levels can facilitate multi-jurisdictional implementation, reducing administrative bottlenecks and ensuring a consistent permitting process across coastal regions[96]. Beyond regulatory challenges, the equitable deployment of e-mCDR must also remain a priority. Many high-potential hubs, including the South, coincide with socially vulnerable communities that could benefit from targeted investment in low-carbon technologies and workforce development initiatives. Policy frameworks should prioritize projects that align with environmental justice initiatives, such as Justice40, to ensure that benefits extend to historically disadvantaged populations.

This study provided a systematic framework for the evaluation and ranking of hubs for e-mCDR deployment via the hybrid pathway, integrating economic, environmental, infrastructural, and social considerations. Although the analysis was specifically designed around the hybrid pathway, the developed framework can be adapted and tailored for other e-mCDR approaches, such as DOC. The primary logistical distinction between the hybrid and DOC pathways lies in their respective infrastructure requirements: the hybrid approach necessitates evaluation of hydrogen management infrastructure, whereas DOC requires comprehensive consideration of CO_2 management infrastructure. In DOC processes, permanent CO_2 storage is essential for process completion; thus, identifying suitable storage sites is a critical component. A detailed assessment of all available CO_2 storage sites across the United States was conducted, and for each hub, primary and alternative storage sites were evaluated based on proximity to deployment locations. The complete analysis, including the detailed list of

storage sites identified for each hub, is provided in Section S7 of the Supplementary Information.

While the analysis provided in this study focused on the U.S. coastal regions, the approach can be extended globally to assess e-mCDR potential in other maritime regions, offering valuable insights for optimizing deployment strategies across diverse geographic and regulatory landscapes. Expanding this framework to international contexts will help identify strategic locations for scaling e-mCDR, enhance cross-border collaboration, and contribute to the broader integration of marine-based CDR in global climate mitigation efforts.

Conclusions

e-mCDR technologies offer a promising route to achieve durable, large-scale carbon removal while co-producing hydrogen, but its deployment could benefit from siting decisions that balance technical, economic, environmental, and social considerations. This work addressed that need by developing and applying a multi-criteria hub-screening framework for the U.S. coastline. The framework integrates facility-level data from 38 coastal sites, using hierarchical clustering to identify candidate hubs and AHP and TOPSIS to rank them, yielding five potential e-mCDR hubs.

By combining five facility-level criteria (CO_2 removal capacity, removal affordability, grid emissions efficiency, local carbon footprint, and social vulnerability index) with two hub-level criteria (facility diversity index and hydrogen management infrastructure), the framework provided an overall characterization of each hub's suitability for e-mCDR deployment. The resulting rankings indicated that the South hub offers particularly high potential, driven by favorable combinations of electricity costs, industrial carbon footprints, and hydrogen infrastructure. Sensitivity analyses on criteria weights and hub composition demonstrated that the overall qualitative ordering of high-, moderate-, and lower-potential hubs is robust to plausible variations in subjective judgments and facility availability, while also highlighting which criteria most strongly influence each hub's performance.

Beyond producing a ranked list of hubs, the analysis clarified how distinct configurations of features create unique e-mCDR hubs. For example, the South and Southeast hubs excel in low-cost energy, whereas West and Northeast excel in large seawater throughputs. This helps developers and policymakers design projects that fit each hub's advantages instead of using a single approach. Although designed for the U.S. and a hybrid mCDR setup, the method can be adapted to other regions and technologies, making it a useful tool for planning carbon removal strategies.

Methodology

Coastal Facilities

Data Collection. A comprehensive database consisting of 38 coastal facilities was generated using a range of publicly available documents[71,73,97–100]. For each facility, key features were recorded, including the facility type (i.e., power plants, desalination plants, or LNG terminals), geolocation, and average intake capacity in million gallons per day (MGD). Features related to the energy infrastructure of the region where the facility is located were also included, such as electricity cost and grid emissions factor. Finally, regional characteristics of the facility's location were considered, including local CO_2 emissions and the social vulnerability index. Table 1 presents the mean with standard deviation (Std), minimum, and maximum values for the collected features. The full database of all 38 facilities, along with a detailed discussion of the features, is provided in Section S2 of the Supplementary Information.

Facilities Criteria Development. The features collected for each facility were used to develop five criteria that influence the facility's suitability as a co-location site for e-mCDR implementation. These criteria include CO_2 removal capacity, removal affordability, grid emissions efficiency, local carbon footprint, and social vulnerability index. These five facility-level criteria were selected to jointly capture the technical potential for CO_2 removal, the economic feasibility of operation, the carbon intensity of the energy supply, and the broader environmental and social context of deployment, thereby enabling a holistic assessment of e-mCDR co-location potential at each site. A detailed justification of feature and criteria selection, along with data sources, is provided in Section S2 of the Supplementary Information. The CO_2 removal capacity of the hybrid pathway depends only on the seawater intake capacity[44]. The hybrid process demonstrates a removal capacity of 4.6 g CO_2 per kilogram of seawater processed as catholyte. When considering a symmetric electrolysis process with equal volume of catholyte and anolyte streams, this translates to an overall removal capacity of 2.3 g CO_2 per kilogram of seawater (52.3 mmol per L of seawater)[44]. Thus, the CO_2 removal capacity of a CDR facility can be simply estimated as the product of the facility's water intake and the hybrid process's removal capacity (2.3 g CO_2/kg seawater). The removal affordability criterion (kg CO_2/\$) is calculated based on the electricity cost in the facility's state (\$/kWh) and the gross energy requirement (kWh/kg CO_2 removed). For example, the gross energy required to remove one kilogram of CO_2 for Equatic's hybrid process is 2.5 kWh per kilogram of CO_2 removed. After accounting for the energy embodied in the co-produced green hydrogen, the net energy intensity is 1.5 kWh per kg of CO_2 removed. In this study, removal affordability is thus used as an electricity-cost-based screening indicator of relative economic favorability across hubs, recognizing that a full lifecycle cost of CO_2 removal (including CAPEX, O&M, and hub-specific infrastructure) would require detailed project-level data that are not consistently available for all 38 facilities. Grid emissions efficiency directly indicates how much electricity is generated for each kilogram of CO_2 released, with higher values indicating a cleaner grid (more energy per unit of CO_2 emitted). Based on the concept of a Specific Intensity Ratio[45], this implies that the average grid emissions efficiency should be higher than 2.5 (kWh/kg CO_2 emitted) to render a net negative carbon removal outcome. The local carbon footprint and social vulnerability index criteria are taken as-is from the extracted data for each facility zip code.

Hubs Identification

Hierarchical clustering. Hierarchical clustering (HC) was used to identify potential e-mCDR hubs along the U.S. coastline, with each hub representing a group of geographically proximate facilities. HC aggregates data points according to their proximity through an iterative process, finally producing a hierarchical structure of clusters[101]. The

Table 1 | Descriptive Statistics of Key Features for Coastal Facilities

	Average intake Capacity (m^3/day) $\times 10^4$	Electricity Cost (cents/kWh)	Grid Emissions Factor ($kgCO_2$/kWh)	Local Carbon Footprint ($kgCO_2$/year/capita)	Social Vulnerability Index (-) [a]
Mean ± Std	240.8 ± 354.2	18.7 ± 4.4	3.9 ± 1.3	15.0 ± 10.1	0.7 ± 0.3
Minimum	0.2	14.9	2.6	8.2	0
Maximum	1134.7	28.1	9.1	42.2	1

Summary statistics of key features collected for 38 coastal facilities identified as potential colocation sites for e-mCDR deployment. The table presents the mean ± standard deviation, minimum, and maximum values for each feature.

[a]Normalized to range between 0 and 1.

clustering process began by calculating the pairwise distances between facilities. The Ward's linkage method with squared Euclidean distances as a measure of similarity[102] was applied to minimize the total within-cluster variance, ensuring that each cluster represented a cohesive group of facilities. Detailed HC procedure is provided in Section S3.1 of the Supplementary Information. A dendrogram was generated to visualize the hierarchical structure and determine the number of clusters based on practical information. Additionally, an effective method is to establish the number of clusters at about $\sqrt{\frac{n}{2}}$ for a dataset of n points[103], which yields 5 clusters with $n = 38$ (i.e., the number of facilities). Cluster validation was conducted using the Elbow method, which plots the within-cluster sum of squares as a function of cluster number[104,105]; the resulting curve exhibited a clear inflection (elbow) at five clusters (Fig. S3 in S3.1.2 in Supplementary Information), supporting the choice of five hubs. Several Python libraries, such as SciPy and matplotlib, were used to perform the HC and output the dendrogram graph, respectively. Additionally, to delineate the geographical boundaries of each identified hub on the map, the Convex Hull algorithm was employed[106] (Section S3.2 of the Supplementary Information). This algorithm constructs the smallest convex polygon that includes all facilities within a given hub, providing a clear visual representation of the hub's spatial extent.

Hubs Criteria Development. Following the identification of hubs using HC, a systematic approach was adopted to quantify and characterize each hub's potential for e-mCDR implementation. Two distinct categories of hub criteria were established. The first category was derived from the corresponding facility criteria, while the second category was based on features extracted specifically at the hub level. For the first category, the hub criteria are calculated as the average values of each criterion of the facilities included in each hub (Eq. 1).

$$C_{j,k} = \frac{\sum_{i=1}^{n} c_{j,i}}{n} \tag{1}$$

where $C_{j,k}$ is the hub-related criterion j for hub k, $c_{j,i}$ is the facility-related criterion j for facility i, and n is the total number of facilities in hub k. Therefore, similar to the facility-level criteria, five criteria were established at the hub level. These include CO_2 removal capacity (ktonne CO_2/day), removal affordability (kg CO_2/\$), grid emissions efficiency, local carbon footprint (Mtonne CO_2/year), and social vulnerability index. As for the second category, two additional hub-level criteria were defined, including the facility diversity index and hydrogen management infrastructure. The facility diversity index quantifies the variety and distribution of different types of facilities (e.g., power plants, desalination plants, LNG terminals) within a hub, which influences logistical flexibility and the robustness of e-mCDR deployment. It was estimated using the Shannon diversity index, a widely used measure for quantifying diversity in a system[107]. For each hub, the diversity score was computed by categorizing the facilities based on their type and calculating the relative proportion of each facility type within the hub (Eq. 2).

$$H' = -\sum_{i=1}^{S} p_i \ln(p_i) \tag{2}$$

where H' is the Shannon diversity index, S is the total number of facility types (in this study: $S = 3$), and p_i is the proportion of each facility type within the hub. A higher diversity score indicates a more balanced distribution of different facility types, whereas a lower score suggests a hub dominated by one or two facility types. Detailed calculations of hub-level criteria are provided in Sections S4.1 and S4.2 of the Supplementary Information.

Hydrogen management infrastructure refers to the availability of transportation, storage, and utilization systems needed to handle co-produced hydrogen via the hybrid approach. The locations of H_2 hubs were compiled using the Department of Energy (DOE) Connect Data tool[74]. To quantify this criterion, a detailed assessment of the hydrogen management infrastructure was conducted. Hydrogen management infrastructure was assessed using the normalized weight of H_2 storage capacity, pipeline length, and total H_2 demand within each hub. Ideally, the presence of hydrogen offtake sites would also be considered; however, the available data was limited. Hubs with more developed infrastructure were assigned higher scores, reflecting their greater suitability for e-mCDR implementation. The Gulf Coast, with its extensive industrial complexes, stands out as a favorable region for its established and accessible hydrogen infrastructure. Further detailed calculations are provided in Section S4.3 in the Supplementary Information.

Criteria Weights Assignment

Following the estimation of criteria values for each hub, the relative significance of these criteria was evaluated. To rank the hubs, it was essential to assign weights to the criteria, which was conducted using the Analytic Hierarchy Process (AHP). AHP is a structured decision-making tool that quantifies the relative importance of multiple factors through pairwise comparisons[108,109]. The criteria were compared according to their importance in assessing the suitability of e-mCDR hubs. Pairwise comparisons were performed using a scale from 1 (equal importance) to 5 (extreme importance), and the values were assigned based on the findings in the literature and consolidated judgments of ten experts with relevant experience in ECC systems, e-mCDR, marine environmental systems, techno-economic analysis, and environmental impact assessment. The resulting pairwise comparison matrix was used to calculate the normalized weights for each criterion by determining the principal eigenvector of the matrix. Consistency of the judgments was evaluated using the consistency ratio (CR), with a CR below 0.1 (in this work, CR = 0.09) indicating acceptable consistency[110]. A detailed AHP procedure is provided in Section S5.1 of the Supplementary Information.

Overall Hub Ranking

Ranking the identified hubs is essential to prioritize locations with the highest potential for successful e-mCDR implementation. For each pathway, the Technique for Order Preference by Similarity to Ideal Solution (TOPSIS) was applied to rank the hubs based on the weighted evaluation criteria[109,111]. This method ranks alternatives by identifying both the positive ideal solution, representing the best possible performance across all criteria, and the negative ideal solution, representing the worst. Criteria values were normalized to ensure comparability across criteria with differing scales. Weighted scores, derived from AHP, were then applied to the normalized values. TOPSIS produces a score between 0 and 1 for each hub, known as the closeness (C) score. This score indicates how close a hub is to the ideal solution, with values closer to 1 being preferable. Hubs closer to the ideal solution received higher rankings, reflecting their overall suitability for e-mCDR implementation. A detailed TOPSIS procedure is provided in Section S5.2 of the Supplementary Information.

Sensitivity Analysis

Sensitivity analysis was conducted on the AHP-derived weights to assess the impact of subjectivity in the pairwise comparison process, which was based on findings in the literature and the authors' expertise. The sensitivity analysis involved systematically adjusting the pairwise comparison scale by increasing the importance of each criterion by a factor of 2 relative to all other criteria, and conversely, decreasing it by a factor of 2. The adjusted weights were then recalculated using AHP, and these new weights were subsequently applied in the TOPSIS method to re-rank the hubs. This process was repeated for each criterion individually. AHP pairwise comparison tables and their respective weights are provided in Section S6 of the Supplementary Information.

Reporting summary

Further information on research design is available in the Nature Research Reporting Summary linked to this article.

Data availability

All data used in this study consist of derived quantitative datasets on coastal facilities, hub-level criteria, and associated environmental, infrastructural, and social indicators for electrochemical marine carbon dioxide removal deployment. These datasets are openly available at https://doi.org/10.6084/m9.figshare.30940202. No additional unpublished data sets were generated.

Code availability

Custom Python code was used to implement the hierarchical clustering. The version of the analysis code used to generate all results and figures has been deposited in a DOI-minting repository and is available at https://doi.org/10.6084/m9.figshare.30940202, together with information on software versions and parameter settings. No restrictions apply to code access.

Received: 15 September 2025; Accepted: 8 January 2026;
Published online: 18 February 2026

References

1. Rogelj, J. et al. Paris Agreement climate proposals need a boost to keep warming well below 2°C. *Nature* **534**, 631–639 (2016).
2. Gür, T. M. Carbon dioxide emissions, capture, storage and utilization: review of materials, processes and technologies. *Prog. Energy Combust. Sci.* **89**, 100965 (2022).
3. Kazlou, T., Cherp, A. & Jewell, J. Feasible deployment of carbon capture and storage and the requirements of climate targets. *Nat. Clim. Change* **14**, 1047–1055 (2024).
4. Pires, J. C. M. Negative emissions technologies: a complementary solution for climate change mitigation. *Sci. Total Environ.* **672**, 502–514 (2019).
5. Breyer, C., Fasihi, M., Bajamundi, C. & Creutzig, F. Direct air capture of CO2: a key technology for ambitious climate change mitigation. *Joule* **3**, 2053–2057 (2019).
6. Rahimi, M., Khurram, A., Hatton, T. A. & Gallant, B. Electrochemical carbon capture processes for mitigation of CO_2 emissions. *Chem. Soc. Rev.* **51**, 8676–8695 (2022).
7. Jeswani, H. K., Saharudin, D. M. & Azapagic, A. Environmental sustainability of negative emissions technologies: a review. *Sustain. Prod. Consum.* **33**, 608–635 (2022).
8. Pradhan, S. et al. Effects of direct air capture technology availability on stranded assets and committed emissions in the power sector. *Front. Clim*. **3**, 660787 (2021).
9. Smith, P. et al. Biophysical and economic limits to negative CO2 emissions. *Nat. Clim. Change* **6**, 42–50 (2016).
10. Wang, T. et al. Characterization of kinetic limitations to atmospheric CO2 capture by solid sorbent. *Greenh. Gases Sci. Technol.* **6**, 138–149 (2016).
11. Hanna, R., Abdulla, A., Xu, Y. & Victor, D. G. Emergency deployment of direct air capture as a response to the climate crisis. *Nat. Commun.* **12**, 368 (2021).
12. Brazzola, N., Meskaldji, A., Patt, A., Tröndle, T. & Moretti, C. The role of direct air capture in achieving climate-neutral aviation. *Nat. Commun.* **16**, 588 (2025).
13. Gutsch, M. & Leker, J. Co-assessment of costs and environmental impacts for off-grid direct air carbon capture and storage systems. *Commun. Eng.* **3**, 1–14 (2024).
14. Jiang, L. et al. Sorption direct air capture with CO2 utilization. *Prog. Energy Combust. Sci.* **95**, 101069 (2023).
15. McQueen, N. et al. A review of direct air capture (DAC): scaling up commercial technologies and innovating for the future. *Prog. Energy* **3**, 032001 (2021).
16. Motlaghzadeh, K., Schweizer, V., Craik, N. & Moreno-Cruz, J. Key uncertainties behind global projections of direct air capture deployment. *Appl. Energy* **348**, 121485 (2023).
17. Mahjour, S. K. & Faroughi, S. A. Risks and uncertainties in carbon capture, transport, and storage projects: a comprehensive review. *Gas. Sci. Eng.* **119**, 205117 (2023).
18. Gholami, R., Raza, A. & Iglauer, S. Leakage risk assessment of a CO2 storage site: a review. *Earth-Sci. Rev.* **223**, 103849 (2021).
19. Lu, J. et al. Fault leakage behaviors and Co2 migration in different types of geological carbon storage. *Chem. Technol. Fuels Oils* **60**, 471–480 (2024).
20. Vidas, H., Hugman, B., Chikkatur, A. & Venkatesh, B. Analysis of the costs and benefits of CO2 sequestration on the U.S. Outer Continental Shelf. (ICF, 2012).
21. Shorey, P. & Abdulla, A. Liquid solvent direct air capture's cost and carbon dioxide removal vary with ambient environmental conditions. *Commun. Earth Environ.* **5**, 1–9 (2024).
22. Li, H. et al. Capturing carbon dioxide from air with charged-sorbents. *Nature* **630**, 654–659 (2024).
23. Aleta, P., Refaie, A., Afshari, M., Hassan, A. & Rahimi, M. Direct ocean capture: the emergence of electrochemical processes for oceanic carbon removal. *Energy Environ. Sci.* **16**, 4944–4967 (2023).
24. Friedlingstein, P. et al. Global Carbon Budget 2022. *Earth Syst. Sci. Data* **14**, 4811–4900 (2022).
25. Gagern, A. & Kapsenberg, L. *Ocean – Based Carbon Dioxide Removal*. (Climate Works Foundation, 2021).
26. Dickson, A. G. The carbon dioxide system in seawater: equilibrium chemistry and measurements. *Guide Best. Pract. Ocean Acidif. Res. Data Rep.* **1**, 17–40 (2010).
27. Committee on Developing a Research Agenda for Carbon Dioxide Removal and Reliable Sequestration et al. *Negative Emissions Technologies and Reliable Sequestration: A Research Agenda*. 25259 (National Academies Press, 2019). https://doi.org/10.17226/25259.
28. Sutherland, B. R. The value of bioenergy sequestration. *Joule* **4**, 2077–2078 (2020).
29. Macreadie, P. I. et al. Blue carbon as a natural climate solution. *Nat. Rev. Earth Environ.* **2**, 826–839 (2021).
30. Boyd, P. W. et al. Mesoscale Iron Enrichment Experiments 1993-2005: synthesis and future directions. *Science* **315**, 612–617 (2007).
31. Zhang, C. et al. Eco-engineering approaches for ocean negative carbon emission. *Sci. Bull.* **67**, 2564–2573 (2022).
32. Eisaman, M. D. Pathways for marine carbon dioxide removal using electrochemical acid-base generation. *Front. Clim*. **6**, 1349604 (2024).
33. Diederichsen, K. M. et al. Electrochemical methods for carbon dioxide separations. *Nat. Rev. Methods Prim.* **2**, 1–20 (2022).
34. Zito, A. M. et al. Electrochemical carbon dioxide capture and concentration. *Chem. Rev.* **123**, 8069–8098 (2023).
35. Hassan, A. et al. Reviving the absorbent chemistry of electrochemically mediated amine regeneration for improved point source carbon capture. *Chem. Eng. J.* **484**, 149566 (2024).
36. Hassan, A., Afshari, M. & Rahimi, M. A membraneless electrochemically mediated amine regeneration for carbon capture. *Nat. Commun.* **16**, 6333 (2025).
37. Afshari, M., Refaie, A., Aleta, P., Hassan, A. & Rahimi, M. A Vanadium redox flow process for carbon capture and energy storage. *ACS EST Eng.* **5**, 1099–1110 (2025).
38. Seo, H., Rahimi, M. & Hatton, T. A. Electrochemical carbon dioxide capture and release with a redox-active amine. *J. Am. Chem. Soc.* **144**, 2164–2170 (2022).
39. Rahimi, M. et al. An electrochemically mediated amine regeneration process with a mixed absorbent for postcombustion CO2 capture. *Environ. Sci. Technol.* **54**, 8999–9007 (2020).
40. Rahimi, M., Zucchelli, F., Puccini, M. & Alan Hatton, T. Improved CO2 capture performance of electrochemically mediated amine regeneration processes with ionic surfactant additives. *ACS Appl. Energy Mater.* **3**, 10823–10830 (2020).

41. Wang, M. et al. Flue gas CO2 capture via electrochemically mediated amine regeneration: system design and performance. *Appl. Energy* **255**, 113879 (2019).
42. Digdaya, I. A. et al. A direct coupled electrochemical system for capture and conversion of CO2 from oceanwater. *Nat. Commun.* **11**, 4412 (2020).
43. Nawaz, S., Lezaun, J., Valenzuela, J. M. & Renforth, P. Broaden research on ocean alkalinity enhancement to better characterize social impacts. *Environ. Sci. Technol.* **57**, 8863–8869 (2023).
44. La Plante, E. C. et al. Electrolytic Seawater mineralization and the mass balances that demonstrate carbon dioxide removal. *ACS EST Eng.* **3**, 955–968 (2023).
45. La Plante, E. C. et al. Saline water-based mineralization pathway for gigatonne-scale CO2 management. *ACS Sustain. Chem. Eng.* **9**, 1073–1089 (2021).
46. Rahimi, M. et al. Carbon dioxide capture using an electrochemically driven proton concentration process. *Cell Rep. Phys. Sci*. **1**, 100333 (2020).
47. Jin, S., Wu, M., Gordon, R. G., Aziz, M. J. & Kwabi, D. G. pH swing cycle for CO2 capture electrochemically driven through proton-coupled electron transfer. *Energy Environ. Sci.* **13**, 3706–3722 (2020).
48. Bui, J. C. et al. Analysis of bipolar membranes for electrochemical CO2 capture from air and oceanwater. *Energy Environ. Sci.* **16**, 5076–5095 (2023).
49. Zhou, M. et al. Mapping the global variation in the efficiency of ocean alkalinity enhancement for carbon dioxide removal. *Nat. Clim. Change* **15**, 59–65 (2025).
50. Wang, H. et al. Simulated impact of ocean alkalinity enhancement on atmospheric CO2 removal in the Bering Sea. *Earths Future* **11**, e2022EF002816 (2023).
51. La Plante, E. C. et al.) 95–100 (Springer Nature Switzerland, Cham, 2024). https://doi.org/10.1007/978-3-031-50244-6_9.
52. Rahimi, M., Catalini, G., Puccini, M. & Alan Hatton, T. Bench-scale demonstration of CO 2 capture with an electrochemically driven proton concentration process. *RSC Adv.* **10**, 16832–16843 (2020).
53. Khoiruddin, K., Wenten, I. G. & Siagian, U. W. R. Advancements in bipolar membrane electrodialysis techniques for carbon capture. *Langmuir* **40**, 9362–9384 (2024).
54. Koivisto, E. S., Reuter, T. & Zevenhoven, R. Performance optimization of bipolar membrane electrodialysis of ammonium sulfate/bisulfate reagents for CO2 mineralization. *ACS EST Water* **3**, 1953–1962 (2023).
55. Kludze, A. et al. Biocement from the ocean: hybrid microbial-electrochemical mineralization of CO2. *iScience* **25**, 105156 (2022).
56. Liu, G., Yang, A. & Darton, R. C. Numerical modeling and comparative analysis of electrolysis and electrodialysis systems for direct air capture. *ACS Sustain. Chem. Eng.* **12**, 3951–3965 (2024).
57. Halloran, P. R. et al. Seawater carbonate chemistry based carbon dioxide removal: towards commonly agreed principles for carbon monitoring, reporting and verification. *Front. Clim*. **7**, 1487138 (2025).
58. Gernaat, D. E. H. J. et al. Climate change impacts on renewable energy supply. *Nat. Clim. Change* **11**, 119–125 (2021).
59. Eisaman, M. D. et al. Indirect ocean capture of atmospheric CO2: part II. Understanding the cost of negative emissions. *Int. J. Greenh. Gas. Control* **70**, 254–261 (2018).
60. Sharifian, R. et al. Electrochemical carbon dioxide capture to close the carbon cycle. *Energy Environ. Sci.* **14**, 781–814 (2021).
61. Ye, X. et al. Arctic oceanic carbon cycle: a comprehensive review of mechanisms, regulations, and models. *Water* **16**, 1667 (2024).
62. Sandhya, S. R., Preston, B., Mohammed, S. & Uvwo, A. Building a CCS Hub at Scale in North America. in *Offshore Technology Conference* D011S002R002 (OTC, 2023).
63. Goldberg, D. S., Nawaz, S., Lavin, J. & Slagle, A. L. Upscaling DAC hubs with wind energy and CO2 mineral storage: considerations for large-scale carbon removal from the atmosphere. *Environ. Sci. Technol.* **57**, 21527–21534 (2023).
64. Meckel, T. A., Bump, A. P., Hovorka, S. D. & Trevino, R. H. Carbon capture, utilization, and storage hub development on the Gulf Coast. *Greenh. Gases Sci. Technol.* **11**, 619–632 (2021).
65. Pezzetti, T., Sou, S. & Pulido, J. *Desalination (Brackish and Seawater) Resource Management Strategy*. https://water.ca.gov/-/media/DWR-Website/Web-Pages/Programs/California-Water-Plan/Docs/RMS/2025/Desalination-RMS---2025.pdf#page=18.37 (2024).
66. Wu, W. & lin, Y. The impact of rapid urbanization on residential energy consumption in China. *PLoS ONE* **17**, e0270226 (2022).
67. Sakmar, S. L. *Energy for the 21st Century: Opportunities and Challenges for Liquefied Natural Gas (LNG*). (Edward Elgar Publishing, 2013).
68. Bondarenko, V. L., Diachenko, O. V. & Diachenko, T. V. Analysis of industrial LNG production technologies. *Chem. Pet. Eng.* **57**, 985–996 (2022).
69. Shi, H. et al. Co-occurrence of California Drought and Northeast Pacific Marine Heatwaves Under Climate Change. *Geophys. Res. Lett.* **48**, e2021GL092765 (2021).
70. Rouleau, T. et al. The Economic Value of America's Estuaries: 2021 Report. *Publications* https://cbe.miis.edu/publications/2 (CBE, 2021).
71. US EPA, O. Emissions & Generation Resource Integrated Database (eGRID). https://www.epa.gov/egrid (EPA, 2020).
72. Justice40 Initiative | Environmental Justice. *The White House* https://bidenwhitehouse.archives.gov/environmentaljustice/justice40/.
73. Greenhouse Gas Inventory Data Explorer | US EPA. https://cfpub.epa.gov/ghgdata/inventoryexplorer/#iallsectors/allsectors/carbondioxide/inventsect/current.
74. Sharma, M. et al. *Carbon Management Projects (CONNECT) Database and Explorer*. https://www.osti.gov/dataexplorer/biblio/dataset/2340723 (2024) https://doi.org/10.18141/2340723.
75. Ruiz Maraggi, L. M. & Moscardelli, L. Hydrogen Storage Potential of U.S. Salt Domes in Texas, Louisiana, and Mississippi. in *The Fourth EAGE Global Energy Transition Conference and Exhibition* 1–5 (European Association of Geoscientists & Engineers, 2023). https://doi.org/10.3997/2214-4609.202321014.
76. Sizaire, P., Lin, B. & Gençer, E. A novel hydrogen supply chain optimization model – Case study of Texas and Louisiana. *Int. J. Hydrog. Energy* **78**, 401–420 (2024).
77. Muthyala, R., Lewis, M. & Deetjen, T. *Integrated Hydrogen Energy Storage System (IHESS) for Power Generation*. https://www.osti.gov/biblio/1884860 (IHESS, 2022).
78. Woo, C. K. et al. Regional revenues of solar and wind generation in Texas. *Energy Policy* **178**, 113586 (2023).
79. Zhang, N., Zheng, J., Song, G. & Zhao, H. Regional comprehensive environmental impact assessment of renewable energy system in California. *J. Clean. Prod.* **376**, 134349 (2022).
80. Balaji, K. & Rabiei, M. Effect of terrain, environment and infrastructure on potential CO2 pipeline corridors: a case study from North-Central USA. *Energy Ecol. Environ.* **6**, 378–393 (2021).
81. Vijayakumar, V., Jenn, A. & Ogden, J. Modeling future hydrogen supply chains in the western United States under uncertainties: an optimization-based approach focusing on California as a hydrogen hub. *Sustain. Energy Fuels* **7**, 1223–1244 (2023).
82. U.S. Energy Information Administration (EIA). Electricity data browser - Net generation for all sectors. https://www.eia.gov/electricity/data/browser/ (2025).
83. Raimi, D., Carley, S. & Konisky, D. Mapping county-level vulnerability to the energy transition in US fossil fuel communities. *Sci. Rep.* **12**, 15748 (2022).

84. Hazboun, S. O. & Boudet, H. S. Public preferences in a shifting energy future: comparing public views of eight energy sources in North America's Pacific Northwest. *Energies* **13**, 1940 (2020).
85. Mills, A. D., Levin, T., Wiser, R., Seel, J. & Botterud, A. Impacts of variable renewable energy on wholesale markets and generating assets in the United States: a review of expectations and evidence. *Renew. Sustain. Energy Rev.* **120**, 109670 (2020).
86. Goldstein, B., Reames, T. G. & Newell, J. P. Racial inequity in household energy efficiency and carbon emissions in the United States: An emissions paradox. *Energy Res. Soc. Sci.* **84**, 102365 (2022).
87. Wendt, A., Sheriff, A., Shih, C. Y., Vikara, D. & Grant, T. A multi-criteria CCUS screening evaluation of the Gulf of Mexico, USA. *Int. J. Greenh. Gas. Control* **118**, 103688 (2022).
88. Ehlig-Economides, C. & Hatzignatiou, D. G. Blue Hydrogen Economy - A New Look at an Old Idea. *(OnePetro* https://doi.org/10.2118/206282-MS (2021).
89. Outlook, W. F. Short-Term Energy Outlook. *Wash. DC August Steo-Full Pdf Wognews Net* (2010).
90. Rahimi, M., Moosavi, S. M., Smit, B. & Hatton, T. A. Toward smart carbon capture with machine learning. *Cell Rep. Phys. Sci*. **2**, (2021).
91. Committee on A Research Strategy for Ocean-based Carbon Dioxide Removal and Sequestration, Ocean Studies Board, Division on Earth and Life Studies & National Academies of Sciences, Engineering, and Medicine. *A Research Strategy for Ocean-Based Carbon Dioxide Removal and Sequestration*. 26278 (National Academies Press, Washington, D.C., 2022). https://doi.org/10.17226/26278.
92. Terlouw, T., Bauer, C., Rosa, L. & Mazzotti, M. Life cycle assessment of carbon dioxide removal technologies: a critical review. *Energy Environ. Sci.* **14**, 1701–1721 (2021).
93. Barr, Z. et al. The permitting, licensing and environmental compliance process: lessons and experiences within U.S. Marine Renewable Energy. *Energies* **14**, 5048 (2021).
94. Hurley, B. M., Oremus, K. L. & Birkenbach, A. M. Testing the waters: the state of U.S. shellfish permitting regulations. *Anim. Front.* **14**, 28–31 (2024).
95. Peiffer, E., Williams, R., Ba-aoum, M., Hudson-Heck, E. & Aranda, I. *Evaluation of New Opportunities for Marine Energy To Power the Blue Economy: Green Hydrogen and Marine Carbon Dioxide Removal*. NREL/SR--5700-89475, 2349050, MainId:90254 https://www.osti.gov/servlets/purl/2349050/ (2024) https://doi.org/10.2172/2349050.
96. Craik, N. Equitable marine carbon dioxide removal: the legal basis for interstate benefit-sharing. *Clim. Policy* 1–15 https://doi.org/10.1080/14693062.2025.2451645 (2025).
97. Electric Power Monthly - U.S. Energy Information Administration (EIA). https://www.eia.gov/electricity/monthly/epm_table_grapher.php.
98. Rayner, N. A. et al. Global analyses of sea surface temperature, sea ice, and night marine air temperature since the late nineteenth century. *J. Geophys. Res. Atmospheres* **108**, 2670 (2003).
99. Sharp, J. D. et al. A mapped dataset of surface ocean acidification indicators in large marine ecosystems of the United States. *Sci. Data* **11**, 715 (2024).
100. CDC. Social Vulnerability Index. *Place and Health - Geospatial Research, Analysis, and Services Program (GRASP)* https://www.atsdr.cdc.gov/place-health/php/svi/index.html (CDC, 2024).
101. Fouché, G. & Langit, L. Introduction to Data Mining. in *Foundations of SQL Server 2008 R2 Business Intelligence* (eds. Fouché, G. & Langit, L.) 369–402 (Apress, Berkeley, CA, 2011). https://doi.org/10.1007/978-1-4302-3325-1_14.
102. Alsulaili, A. D. & Alshawish, S. Spatial and temporal multivariate statistical analysis to assess drinking water quality in medical services. *J. Eng. Res*. **9**, 11035 (2021).
103. Han, J., Kamber, M. & Pei, J. 10 - Cluster Analysis: Basic Concepts and Methods. in *Data Mining (Third Edition)* (eds. Han, J., Kamber, M. & Pei, J.) 443–495 (Morgan Kaufmann, Boston, 2012). https://doi.org/10.1016/B978-0-12-381479-1.00010-1.
104. Shi, C. et al. A quantitative discriminant method of elbow point for the optimal number of clusters in clustering algorithm. *EURASIP J. Wirel. Commun. Netw.* **2021**, 31 (2021).
105. Syakur, M. A., Khotimah, B. K., Rochman, E. M. S. & Satoto, B. D. Integration K-Means clustering method and elbow method for identification of the best customer profile cluster. *IOP Conf. Ser. Mater. Sci. Eng.* **336**, 012017 (2018).
106. Linh, N. K. & Muu, L. D. A convex Hull algorithm for solving a location problem. *RAIRO - Oper. Res.* **49**, 589–600 (2015).
107. DeJong, T. M. A comparison of three diversity indices based on their components of richness and evenness. *Oikos* **26**, 222–227 (1975).
108. Saaty, T. L. How to make a decision: the analytic hierarchy process. *Eur. J. Oper. Res.* **48**, 9–26 (1990).
109. Goh, H. H. et al. Combination of TOPSIS and AHP in load shedding scheme for large pulp mill electrical system. *Int. J. Electr. Power Energy Syst.* **47**, 198–204 (2013).
110. Feizabadi, A. et al. MCDM selection of pulse parameters for best tribological performance of Cr–Al2O3 nano-composite co-deposited from trivalent chromium bath. *J. Alloy. Compd.* **727**, 286–296 (2017).
111. Yoon, K. P. & Hwang, C.-L. *Multiple Attribute Decision Making: An Introduction*. (SAGE Publications, 1995).

Acknowledgements

Dr. Rahimi acknowledges the support from the NSF CAREER (Award #: 2338664), the Department of Energy (DOE; Award #: DE-FE-0032408), and the University of Houston High Priority Area Research Seed Grant (Award #: I0511686).

Competing interests

There is potential competing interest, as ELP, DJ, and GS are co-founders of Equatic. All other authors declare no competing interests.

Additional information

Supplementary information The online version contains supplementary material available at https://doi.org/10.1038/s44458-026-00035-9.

Correspondence and requests for materials should be addressed to Mim Rahimi.

Peer review information *Communications Sustainability* thanks the anonymous reviewers for their contribution to the peer review of this work. Primary Handling Editor: Nandita Basu. [A peer review file is available].